

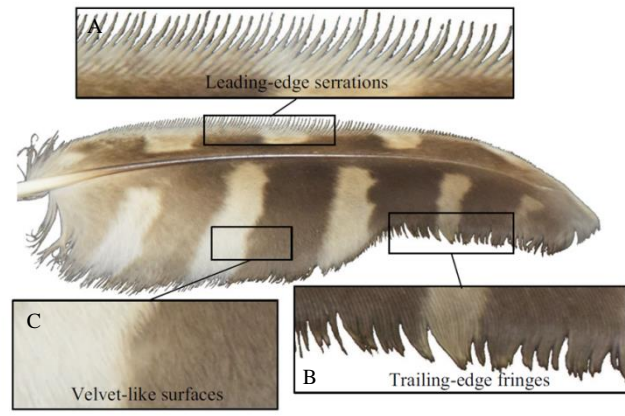


# Owl's leading-edge serrations hold a key to achieve silent flight

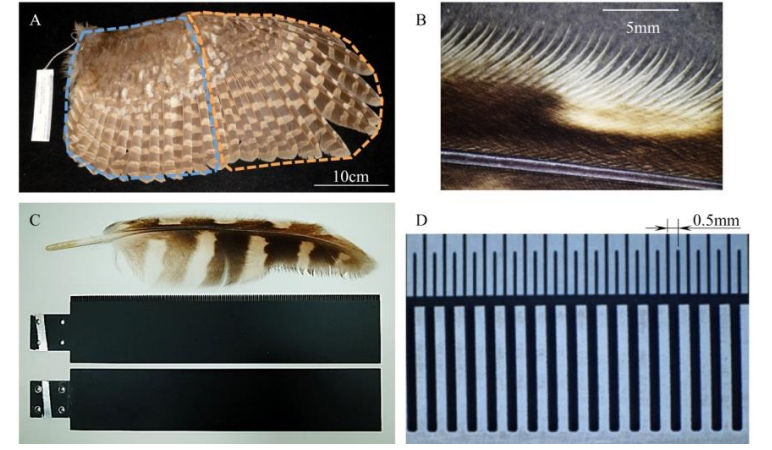
## Introduction: Owl – The Silent Hunter



Owls are widely known for silent flight, achieving remarkably low noise gliding and flapping flights owing to their unique wing morphologies, which are normally characterized by leading-edge serrations (A), trailing-edge fringes (B) and velvet-like surfaces (C). However, how these morphological features affect aerodynamic force production and sound suppression is still not well known. Here we address an integrated study of owl-inspired wing models with and without leading-edge serrations through large-eddy simulations (LES) and wind tunnel experiments to unveil the novel mechanisms associated with tradeoff between aerodynamic force production and sound suppression.

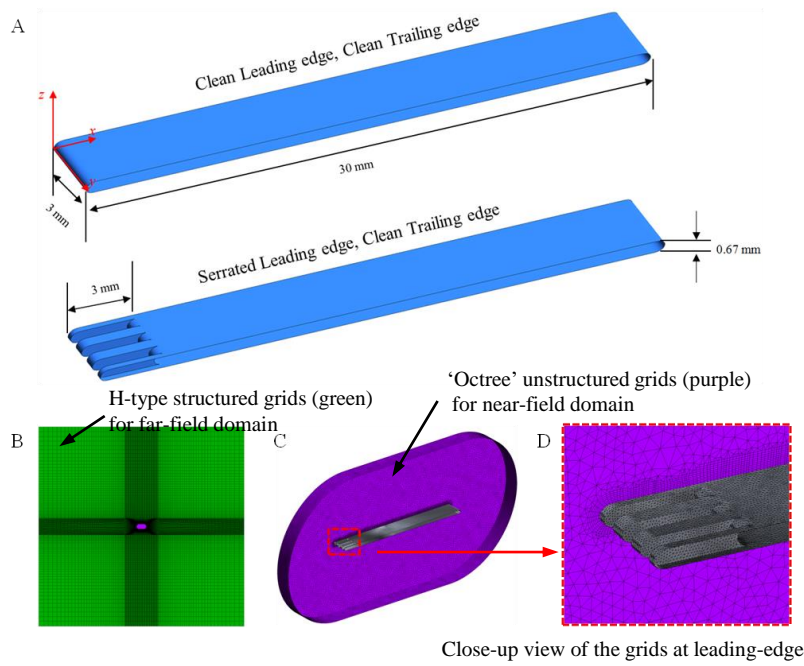


## Material: Owl-inspired single-feather wing model



(A) Right wing of a female ural owl. (B) The comb-like serrated leading-edge. (C) Owl single feather (top)-inspired wing models with serrated (middle) and clean (bottom) leading-edge. (D) Close-up view of the serrations.

## Method: Large eddy simulation using WALE model



Filtered governing equations for incompressible flows

$$\frac{\partial \bar{U}_i}{\partial x_i} = 0 \quad \frac{\partial \bar{U}_i}{\partial x_j} + \frac{\partial \bar{U}_j}{\partial x_i} = -\frac{1}{\rho} \frac{\partial \bar{p}}{\partial x_j} + \frac{\partial}{\partial x_j} \left( \frac{\tau_{ij}}{\rho} \right) + \frac{\partial}{\partial x_j} \left( \frac{\tau_{ij}^s}{\rho} \right) + \frac{\partial}{\partial x_j} \left( \frac{\tau_{ij}^b}{\rho} \right)$$

subgrid-scale stress tensor  $\tau_{ij}$  accounts for the influence of the filtered small scale eddies

$$\tau_{ij} = \overline{U_i U_j} - \overline{U_i} \overline{U_j}$$

an eddy-viscosity assumption to close the  $\tau_{ij}$  term

$$\tau_{ij} = \frac{2}{3} \overline{u'v'w'} \delta_{ij} - 2\nu_t \overline{S_{ij}} \quad \delta_{ij} \text{ the Kronecker symbol}$$

$\nu_t$  the turbulent eddy viscosity

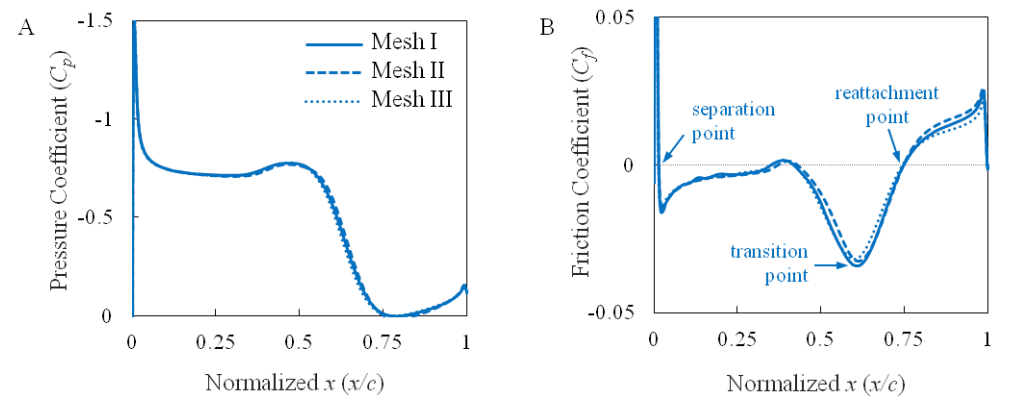
$\overline{S_{ij}}$  the strain rate tensor of the resolved field defined by

$$\overline{S_{ij}} = \frac{1}{2} \left( \frac{\partial \bar{U}_i}{\partial x_j} + \frac{\partial \bar{U}_j}{\partial x_i} \right)$$

Wall-adapted local eddy-viscosity (WALE) model

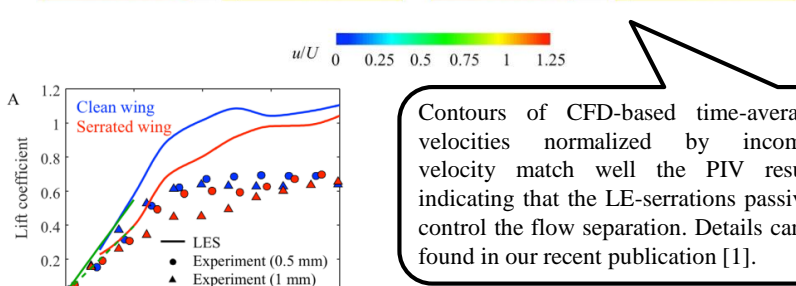
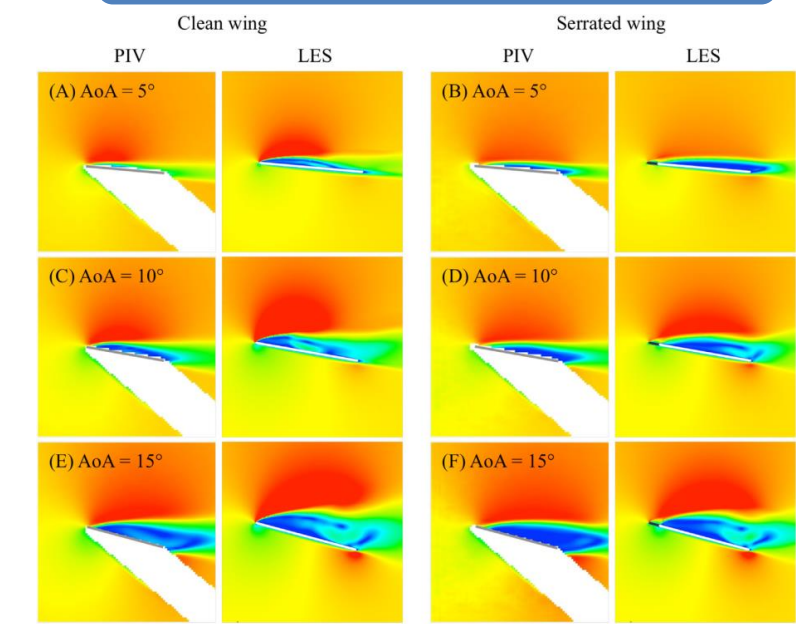
$$\nu_t = (C_D D)^2 \frac{(S_{ij}^2 S_{kl}^2)^{1/2}}{(S_{ij}^2 S_{kl}^2)^{1/2} + (S_{ij}^2 S_{kl}^2)^{1/4}} \quad S_{ij}^2 = \frac{1}{2} \left( \frac{\partial \bar{U}_i}{\partial x_j} + \frac{\partial \bar{U}_j}{\partial x_i} \right)^2 \quad S_{kl}^2 = \frac{1}{3} \left( \frac{\partial \bar{U}_k}{\partial x_l} + \frac{\partial \bar{U}_l}{\partial x_k} \right)^2$$

## Grid sensitivity study: clean model in steady case $U = 3 \text{ m/s}$ $\text{AoA} = 5 \text{ deg}$



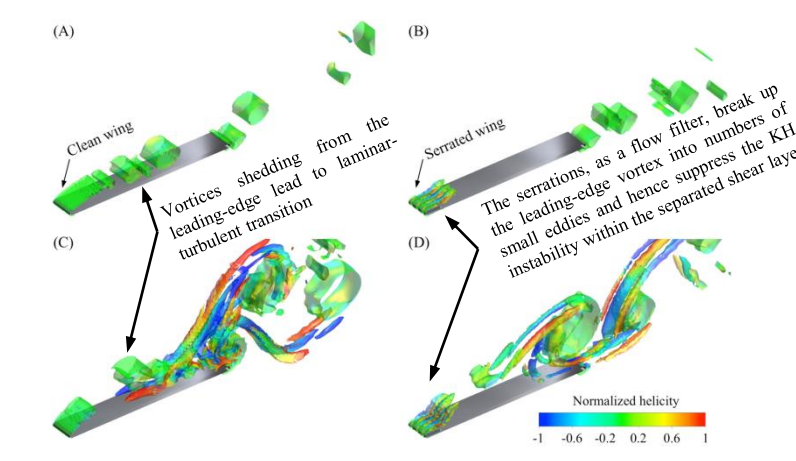
	Mesh I	Mesh II	Mesh III
Minimum grid spacing	0.025 mm	0.050 mm	0.075 mm
Node number of the inner domain	691,042	502,622	308,275
Separation position (x/c)	$1.340 \times 10^{-2}$	$1.358 \times 10^{-2}$	$1.206 \times 10^{-2}$
Transition position (x/c)	$6.058 \times 10^{-1}$	$6.124 \times 10^{-1}$	$5.981 \times 10^{-1}$
Reattachment position (x/c)	$7.478 \times 10^{-1}$	$7.461 \times 10^{-1}$	$7.429 \times 10^{-1}$

## Steady case: $U_{inlet} = U = 3 \text{ m/s}$



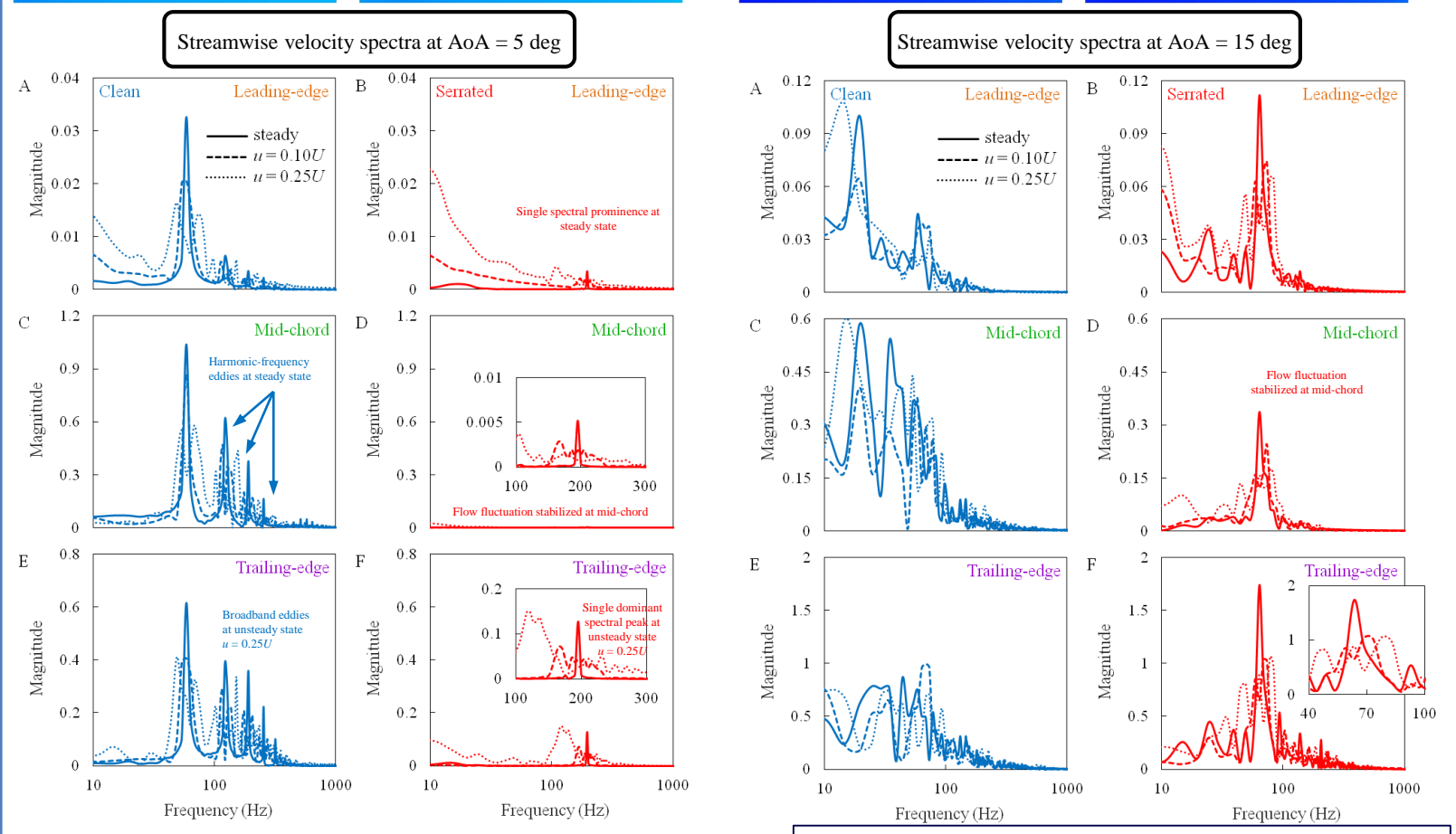
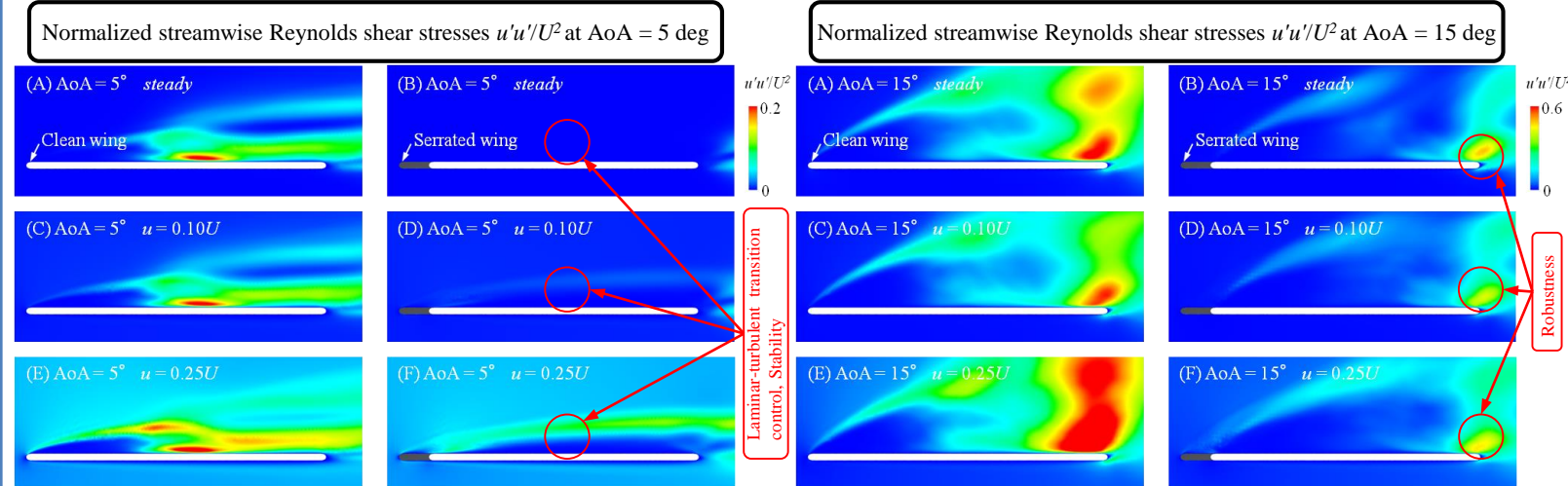
Contours of CFD-based time-averaged velocities normalized by incoming velocity match well the PIV results, indicating that the LE-serrations passively control the flow separation. Details can be found in our recent publication [1].

Lift-to-drag ratios are in reasonable agreement between EXP and CFD whereas both lift and drag are over-predicted in CFD due to 3D effect owing to interplay among wing tip vortex, leading- and trailing-edge vortices for low aspect ratio wings (AR = 5). Green solid line (lift-curve slope estimated by 2D thin airfoil theory) and green dashed line (lifting-line theory for 3D plate) match well the LES and EXP results, respectively, further validating the LES-based simulations.



## Unsteady case: $U_{inlet} = U + u \cdot \sin(2\pi ft)$

$$u = 0.10U, 0.25U, f = 5 \text{ Hz}$$



LE-serrations are capable of stabilizing the flow fluctuations due to laminar-turbulent transition and providing a robust mechanism in resolving the tradeoff between sound suppression and force production.

## Conclusions

1. Leading-edge serrations, as a flow filter, can break up the leading-edge vortex into small eddies and hence suppress the KH instability within the separated shear layer.
2. Leading-edge serrations can passively control laminar-turbulent transition through stabilizing suction flow, which is robust and effective even under unsteady state in suppressing sound production.
3. Leading-edge serrations are capable of providing a strategy in resolving the tradeoff between sound suppression and force production. Compared to the clean model, the serrated wing model shows a reduction in aerodynamic force production at lower AoAs < 15 deg, but obviously a capability to achieve an even aerodynamic performance at higher AoAs > 15 deg while suppressing the noise production.
4. Owl-inspired leading-edge serrations may provide a useful device for aero-acoustic control in biomimetic rotor designs for wind turbines, aircrafts, multi-rotor drones as well as other fluid machinery.

## Publication

Scan the QR code to access

[1] Chen Rao et al 2017 *Bioinspir. Biomim.* 12 046008 (press released)